HYDROLOGICAL PROCESSES
Hydrol. Process. **16**, 2645–2666 (2002)
Published online 18 April 2002 in Wiley InterScience (www.interscience.wiley.com). DOI: 10.1002/hyp.1064

System dynamics model for predicting floods from snowmelt in North American prairie watersheds

L. Li and S. P. Simonovic*
Department of Civil and Environmental Engineering, The University of Western Ontario, London, Ontario, Canada N6A 5B9

Abstract:

This study uses a system dynamics approach to explore hydrological processes in the geographic locations where the main contribution to flooding is coming from the snowmelt. Temperature is identified as a critical factor that affects watershed hydrological processes. Based on the dynamic processes of the hydrologic cycle occurring in a watershed, the feedback relationships linking the watershed structure, as well as the climate factors, to the streamflow generation were identified prior to the development of a system dynamics model. The model is used to simulate flood patterns generated by snowmelt under temperature change in the spring. Model structure captures a vertical water balance using five tanks representing snow, interception, surface, subsurface and groundwater storage. Calibration and verification results show that temperature change and snowmelt play a key role in flood generation. Results indicate that simulated values match observed data very well. The goodness-of-fit between simulated and observed peak flow data is measured using coefficient of efficiency, coefficient of determination and square of the residual mass curve coefficient. For the Assiniboine River all three measures were in the interval between 0·92 and 0·96 and for the Red River between 0·89 and 0·97. The model is capable of capturing the essential dynamics of streamflow formation. Model input requires a set of initial values for all state variables and the time series of daily temperature and precipitation information. Data from the Red River Basin, shared by Canada and the USA, are used in the model development and testing. Copyright © 2002 John Wiley & Sons, Ltd.

KEY WORDS flood; system dynamics; hydrologic dynamics; feedback; watershed

INTRODUCTION

Flood is a hydrological phenomenon characterized by both precipitation and soil-water contributions. However, snowpack accumulation and melt are regarded as important sources of runoff and contribute significantly to the cause of floods in North America (World Meteorological Organization, 1970; Gray and Male, 1981). In order to forecast snowmelt runoff, an understanding of the hydrological processes in the watershed and their response to external inputs are needed because they are both influenced by the internal structure of the watershed system as well as by external disturbances. Estimation of snowmelt and carrying capacity of the watershed system depends greatly on the availability of the climatic and landscape data required for snowmelt runoff computation. Hence, the proper system description methodology and the appropriate prediction techniques are required for practical use in estimating snowmelt runoff.

Considerable effort has been made to investigate and describe the runoff generation process. Simulation models have been utilized as powerful tools either for generating streamflow or determining how runoff responds to the change in climate, landscape and soil-water saturation. A simple way to predict water flow is by using statistical approaches (Thomas and Megahan, 1998). They are useful in the analysis of relations between water flow and relevant conditions in a simple system, but are incapable of capturing important non-linear hydrological processes. Jakeman and Hornberger (1993) used time series techniques for estimating

* Correspondence to: S. P. Simonovic, Department of Civil and Environmental Engineering, The University of Western Ontario, London, Ontario, Canada N6A 5B9. E-mail: simonovic@uwo.ca

Received 21 February 2001
Accepted 6 September 2001

transfer functions that describe the relationship between precipitation and streamflow. However, the runoff time series do not contain much information on the interactions among external actors and internal elements of the catchment system. More complex runoff models (Bobba and Lam, 1990; Arp and Yin, 1992; Kite *et al*., 1994) were developed to route water through different land-use, soil-levels and evapotranspiration processes. These models can test how water flow responds to the varying conditions, but a large amount of information, which is not always available, is required. Neural networks, as predictive tools, are also used to predict runoff (Hsu *et al*., 1995; Lealand *et al*., 1999; Ehrman *et al*., 2000). Neural networks provide a mathematically valid, pattern recognition technique to produce complex algorithms describing the interrelationships among a number of input and output variables (Rumelhardt and McClelland, 1986). They are useful for dealing with abundant data with non-linear and seasonal tendencies, but are not easily applied to analyse cause–effect relationships (Rumelhardt and McClelland, 1986).

Some existing hydrological models also took snowpack accumulation and melt into consideration, such as the Hydrological Simulation Program–Fortran (Bicknell *et al*., 1997), Precipitation-Runoff Modeling System (Leavesley *et al*., 1983), Hydrological Simulation Model (Manley, 1978), MIKE 11 flood forecasting system (Danish Hydraulic Institute, 1992), the SLURP (Kite, 1998) and HBV hydrological model (Lindström *et al*., 1997). These models integrate climatic factors, snowpack and soil components. More data may be required on climate, landscape and soil properties for calibrating these models.

The degree-day method is generally considered to be a good approach to calculating snowmelt (US Army Corps of Engineers, 1971; Anderson, 1973). It provides a simple way to estimate snowmelt on the basis of air temperature. The method has been applied to estimate the streamflow from snowmelt (Martinec, 1960, 1970, 1975; Anderson, 1973; Singh and Kumar, 1996). Runoff is routed as a part of snowmelt in the models, but the dynamics of moisture movement and saturation within soil layers is ignored.

The contribution of snowmelt to runoff varies with interactions among climatic factors, vegetation, soil physical properties and moisture saturation. Most major floods occur following heavy precipitation in the previous fall, substantial snowfall, sudden thaws in association with heavy rainfall or wet snow conditions during the spring break-up. Precipitation and temperature are two key factors affecting flood events. Snowmelt water and/or rainfall will partially be intercepted by vegetation, and some infiltrated to soil. Interception capacity is subject to seasonal change of vegetation. Vegetation growth within a year is for biomass to accumulate in time and space until achieving the maximum biomass and cover that is consistent with the local physical environment (Gutierrez and Fey, 1980). Vegetation increases rapidly during spring, then reaches its maximum value and eventually decreases as the growth rate approaches zero. Infiltration rate and surface storage capacity depend on the soil physical conditions. In the snowmelt active season, vegetation is rare and the infiltration rate is limited due to the frozen surface soil. These conditions often result in flooding. The active temperature ($\geq 0\,^{\circ}\mathrm{C}$) and its duration period are important for vegetation growth and surface soil defrosting and refreezing. When modelling snowmelt runoff, it is needed to represent this phenomenon properly.

The existing hydrologic models have been applied for either generating streamflow or determining runoff response to the external change. However, an analysis of the endogenous feedback structure of a watershed system that generates and regulates dynamic hydrologic behaviour is not addressed in the existing models. Also, the canopy interception capacity and the impact of temperature on soil infiltration rate in most models are assumed to be constant. These assumptions ignore the impact of temperature fluctuations on both the vegetation growth dynamics and the change of soil physical states, which has significant impact on hydrological dynamics. Therefore, this study attempts to develop a dynamic model for addressing flood generation from snowmelt associated with hydrological processes. The model considers temperature as a critical external factor to determine canopy interception capacity and physical state of the soil. System dynamics is applied as a methodology that provides an inside view of endogenous feedback structures relating to hydrological processes. The model developed in this study captures the essential dynamic characteristics of surface and subsurface hydrological processes that are non-linear, occur in the feedback form and include time delays. Based on the analysis and integration of existing information available on hydrological processes occurring in a watershed, the paper first outlines the general components of the watershed system. Then, a dynamic

hypothesis to generate hydrological dynamics is developed from the feedback relations among the components. Referring to existing knowledge and information, the model is formulated using mathematical equations and implemented using the STELLA II simulation tool (High Performance Systems, 1997). The model is calibrated and verified by the historical flood events occurring in the Assiniboine and the Red River basins, Manitoba, Canada. The paper finally discusses model application issues and ends with conclusions.

MODEL DEVELOPMENT

Description of hydrological processes

Lumped or integrated approaches have a long tradition in hydrological modelling (Beven, 2001), because they can effectively use available daily data related to runoff records, long and reliable records of precipitation and temperature. A lumped parameter conceptual model could be capable of simulating the various components of streamflow. This research builds on the existing models and integrates climatic factors and hydrological processes. Model parameters are defined for the whole watershed and the simulation of vertical water balance using five tanks representing (a) snow storage, (b) canopy storage, (c) surface soil storage, (d) subsurface soil storage, and (e) groundwater storage is performed. Figure 1 shows that any precipitation falling as snow is accumulated in snow storage. Precipitation as rainfall and water from snowmelt first enter into canopy storage.

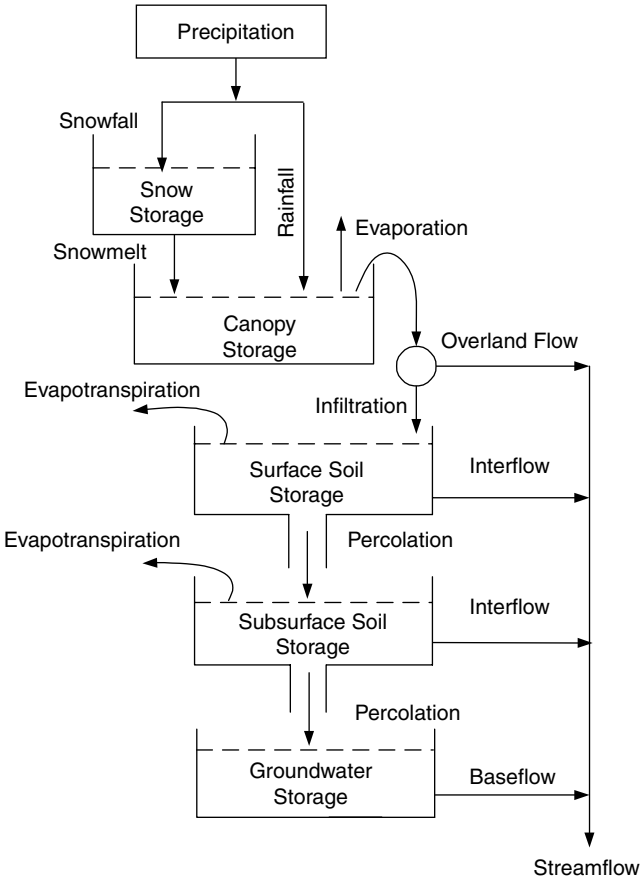

Figure 1. A schematic representation of the vertical water balance

Canopy storage represents the interception of moisture by vegetation and varies with seasonal change due to the vegetation growth. The loss from this storage is due to evaporation. Any moisture in excess of the canopy storage maximum capacity is passed to the surface soil storage. There is a limit on the rate at which moisture can enter the surface soil storage. The limit is a function of the surface soil conditions and soil moisture content. Temperature critically determines the soil physical state, and existing soil water saturation in the form of feedback affects the infiltration. The difference between the volume of water from canopy storage and the amount infiltrated into the soil becomes overland flow into the river.

Losses from the surface soil storage include evapotranspiration, interflow and percolation to the subsurface soil storage. Evapotranspiration flux aggregates physical (evaporation) and biological loss (transpiration). It is dependent on moisture saturation and weather conditions. Interflow (i.e. lateral flow) is a very complex function of the effective horizontal permeability, water saturation and availability, the gradient of the layer and the distance to a channel or land drain. Percolation to the lower layer is dependent on the water saturation within the surface and subsurface soil layers.

Subsurface soil storage represents moisture below the surface layer but still in the root zone. Water enters this layer by percolation from surface soil. Similar losses to those in surface soil storage exist in the subsurface soil storage: evapotranspiration, interflow runoff and percolation to groundwater. Evapotranspiration from the subsurface soil layer depends on vegetation transpiration and varies with vegetation type, the depth of rooting, density of vegetation cover, and the stage of plant growth along with the moisture characteristics of the soil zone. Interflow and percolation to groundwater storage may depend on moisture saturation. Groundwater storage as an infinite linear reservoir continuously contributes to the runoff. Subsurface interflow and baseflow from groundwater are important contributions to the streamflow, especially in a dry or winter season. Their contribution to the streamflow is very dependent on the spatio-temporal characteristics of the watershed, especially in the topography, effective horizontal permeability, the gradient of the layer and the distance to a channel or land drain.

Based on the above analysis, temperature is presented as an important climate factor that influences snowpack accumulation and snowmelt as well as the soil and water physical states. The runoff and flood generation from snowmelt may follow a general pattern as temperature changes during the active snowmelt period. In the winter period, precipitation is accumulated as the snowpack due to low temperature, and the runoff contribution mostly comes from the groundwater and subsurface soil storage due to the frozen surface soil. As temperature reaches an active point in the early spring, snow starts melting. Most of the snowmelt becomes overland flow, owing to the small canopy storage and the frozen surface soil. As temperature increases, snowmelt generates more water, which rapidly increases the streamflow and gradually leads to flood flows. In the meantime, active temperature also gradually defrosts soil, therefore increasing the infiltration rate and the surface soil storage capacity. As a result, the streamflow starts to decline. If heavy rain occurs during the snowmelt period, the streamflow will rise more rapidly and the peak magnitude will be larger. As the accumulated snowpack melts, the streamflow gradually returns to normal level. After the snowmelt period, main streamflow contributions will come from the groundwater and the soil storage. Fluctuations in the streamflow depend strongly on the rainfall magnitude. This pattern has been clearly observed in different locations along the Assinibione River and the Red River in Manitoba, Canada.

Dynamic hypothesis

System dynamics, a feedback-based methodology, is applied to develop the hydrologic model that represents the dynamics of hydrologic processes described above. S provides a conceptual framework useful in the assembly of non-linear differential equations with complex feedback (Forrester, 1968). It recognizes that the dynamic behaviour of systems is controlled by the feedback loop structure (Senge, 1990; Richardson, 1991). A positive feedback stimulates all factors in a loop to increase or decrease. A negative feedback loop tends to keep elements in equilibrium. When any of the factors in a negative feedback loop are removed from the equilibrium state, the negative feedback will force it back to equilibrium. A system dynamics approach helps

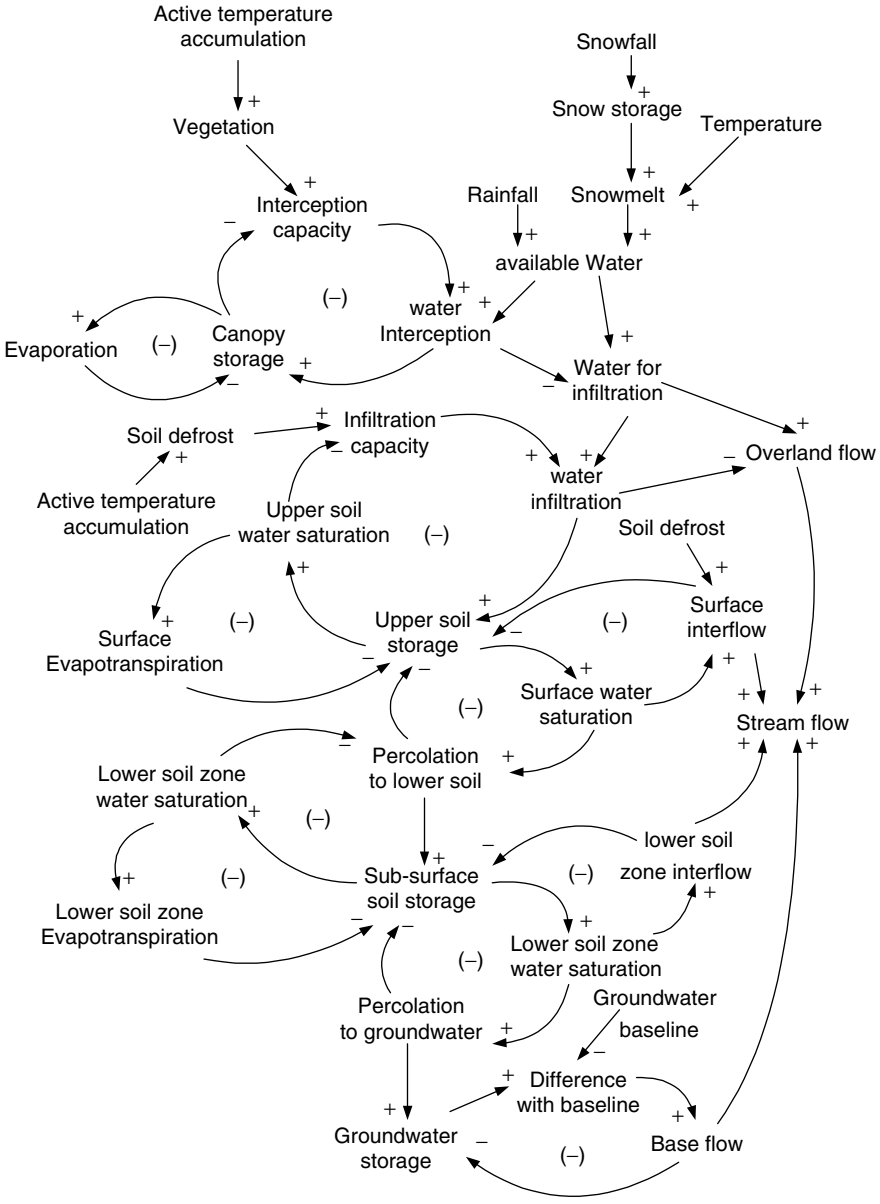

Figure 2. Basic dynamic hypothesis of hydrological dynamics in a watershed

in the identification of the sources of problem behaviour and the understanding of the feedback structure of the system. From the viewpoint of the system dynamics, the dynamic behaviour of the hydrologic system is dominated by the feedback loop structure, which controls change in the system. As external and internal conditions vary, the contribution of each feedback loop may change, and the dominance in controlling internal moisture dynamics may shift from one feedback loop to another. Hence, an integrated analysis of complex feedback relationships could be helpful for a better understanding of the watershed hydrologic dynamics. Based on the hydrologic processes in surface–subsurface layers, a basic dynamic hypothesis to generate hydrological dynamics is developed (Figure 2). The basic dynamic hypothesis shows that the feedback structure of the

fundamental state variables is related to hydrological flow processes as well as exogenous factors. The strength of each hydrological flow process is represented by a rate variable. Linking state variables to rate variables, feedback loops can be formed to control the hydrological behaviour. When rainfall, or snowmelt water enters into the system, the hydrologic flow processes are regulated by those feedback loops. There is one negative feedback loop that controls canopy capacity and water interception.

(1) Water interception +> Canopy storage −> Interception capacity +> Water interception.

The signs in above loop, '+' and '−', represent the positive or negative relationships between the first variable and the next one. Loop (1) shows that water interception by canopy increases water in the canopy storage, which reduces the interception capacity, and finally limits water interception rate. Interception capacity is dependent on the vegetation cover, which is subjected to active temperature accumulation during the snowmelt active period. Negative feedback loops controlling surface soil storage can be traced as follows.

(2) Water infiltration +> Surface soil storage +> Surface soil water saturation −> Infiltration capacity +> Water infiltration.
(3) Surface soil storage +> Surface soil water saturation +> Evapotranspiration −> Surface soil storage.
(4) Surface soil storage +> Surface soil water saturation +> Percolation to subsurface soil −> Surface soil storage.
(5) Subsurface storage +> Subsurface soil water saturation −> Percolation to subsurface soil +> Subsurface storage.
(6) Surface soil storage +> Surface soil water saturation +> Surface soil interflow −> Surface soil storage.

Loop (2) describes the source of water for surface soil storage. Water infiltration through the surface soil increases the water saturation, which further limits infiltration into the surface soil. Loop (3) describes the evapotranspiration process. Loops (4) and (5) explain that the percolation of water to the subsurface storage is dependent on the water saturation in the surface and subsurface soil layers. Loop (6) describes the surface soil interflow, which is influenced by the saturation level. Loops (2) to (6) are strongly regulated by temperature during snowmelt active periods when the surface soil is frozen. Frozen surface soil limits water infiltration rate and water availability for evapotranspiration, percolation and interflow. The following negative loops are identified to control moisture losses from the subsurface soil storage.

(7) Subsurface soil storage +> Subsurface soil water saturation +> Evapotranspiration −> Subsurface soil storage.
(8) Subsurface soil storage +> Subsurface soil water saturation +> Subsurface soil interflow −> Subsurface storage.
(9) Subsurface soil storage +> Subsurface soil water saturation +> Percolation to groundwater −> Subsurface soil storage.

Loops (7) to (9) show that evapotranspiration, interflow and percolation processes are determined by the subsurface soil storage saturation. Groundwater storage is assumed to behave as a shallow reservoir, and baseflow is determined by

(10) Groundwater storage +> Difference from the groundwater baseline +> Base flow −> Groundwater storage.

The above dynamic hypothesis shows that the rainfall and the snowmelt are the most important external water sources affecting the water balance between the soil layers and the groundwater storage. Internal hydrologic processes and negative feedback structures among the soil layers and the groundwater reservoir

provide internal storage buffers and adjustment mechanisms that reduce or delay the impact of the external disturbance on the streamflow. The main role of negative feedback structures is to maintain the system balance. Floods occur when the external water volume exceeds internal storage buffers and its adjustment capacity.

Model formulation

Based on the vertical water balance (Figure 1), a mathematical representation of the model is formulated as below.

Snow storage sector. Any precipitation falling as snowfall is accumulated in the snow storage. A critical temperature is used to determine whether the measured or forecasted precipitation is rainfall or snowfall (Martinec *et al.*, 1983). Snowmelt rate can be calculated by the degree-day factor (Martinec, 1960, 1970, 1975; Anderson, 1973; Singh and Kumar, 1996). On the basis of water balance, the snow storage change rate can be expressed mathematically as:

$$\frac{\mathrm{d}S1}{\mathrm{d}t} = P_s c_1 - \alpha T \tag{1}$$

where $S1$ (cm) represents the water in snow storage, P_s (cm day^{-1}) is precipitation as snowfall identified by a critical temperature, c_1 (cm snow/cm precipitation) is snow-water equivalent coefficient, α is (cm $^{\circ}$C^{-1} day^{-1}) the degree-day factor for snowmelt, and T ($^{\circ}$C) is daily mean temperature.

Canopy storage sector. Canopy interception rate is dependent on the canopy interception capacity, existing water in the canopy storage, and the availability of water from snowmelt and rainfall. Water loss in canopy storage is due to the evaporation, which is assumed to depend on air temperature when intercepted water is available for evaporation. The water balance equation for the canopy storage and the interception rate can be written as:

$$\frac{\mathrm{d}S2}{\mathrm{d}t} = R_{CI} - c_2 T \tag{2}$$

$$R_{CI} = \min[(\alpha T/c_1 + P_r), (C_{CI} - S2)] \tag{3}$$

where $S2$ (cm) represents the water in the canopy storage, R_{CI} (cm day^{-1}) stands for canopy interception rate, c_2 (cm $^{\circ}$C day^{-1}) is an evaporation coefficient, P_r (cm day^{-1}) is precipitation as rainfall and C_{CI} represents canopy interception capacity.

C_{CI} varies with the seasonal growth of vegetation. During the winter season, the canopy interception capacity is very small, since the leaves have fallen from the trees and grasses are waded. In a normal biological growth pattern, canopy growth follows an S-curve pattern, i.e. with rise in temperature, plants start growing, and the growth increases as the temperature increases until it reaches maximum. In order to represent this process, active temperature accumulation is taken as an index to estimate the change of canopy interception capacity:

$$C_{CI} = C_{max}(C_{min} + C_{tc}) \tag{4}$$

$$C_{tc} = \begin{cases} \left[\left(\sum T\right) \Big/ T_{C_{max}}\right]^{c_c} & \text{if} \quad \sum T < T_{C_{max}} \\ 1 & \text{if} \quad \sum T \geq T_{C_{max}} \end{cases} \tag{5}$$

where C_{max} (cm /day^{-1}) is the maximum C_{CI}, C_{min} (dimensionless) is the minimum of C_{max} during the winter, C_{tc} (dimensionless) is the influence of active temperature accumulation on the canopy size, c_c is an exponential coefficient of active temperature accumulation on the canopy growth, and $T_{C_{max}}$ is the maximum active temperature accumulation point at which canopy storage reaches a maximum.

Surface soil storage sector. Moisture change in the surface soil storage depends on infiltration, evapotranspiration, interflow and percolation. Evapotranspiration, interflow and percolation from the surface soil are determined by the climatic conditions, water saturation, and water availability (Manley, 1982; Bicknell *et al.*, 1997). Water availability is influenced by water available from the canopy storage and can be expressed as a function of active temperature. Therefore, the change of water in the surface soil storage is determined by:

$$\frac{dS3}{dt} = R_I - R_{E1} - R_{F1} - R_{P1} \tag{6}$$

$$R_I = \min[(\alpha T/C_1 + P_r) - R_{CI}, I_l] \tag{7}$$

$$R_{E1} = c_3 T S_{ms}^{\lambda} C_{ti} \tag{8}$$

$$R_{F1} = c_4 S_{ms}^{\lambda} C_{ti} \tag{9}$$

$$R_{P1} = \begin{cases} c_5 (S_{ms} - S_{mss})^3 C_{ti} & \text{if} \quad S_{ms} - S_{mss} > 0{\cdot}01 \\ 0 & \text{if} \quad S_{ms} - S_{mss} \le 0{\cdot}01 \end{cases} \tag{10}$$

where $S3$ (cm) is the water in surface soil storage, R_I, R_{E1}, R_{F1} and R_{P1} (cm day^{-1}) are the rates of infiltration, evapotranspiration, interflow and percolation respectively in surface soil storage, I_l is the soil infiltration limit, c_3 (cm °C^{-1} day^{-1}) is an evapotranspiration coefficient, S_{ms} and S_{mss} (dimensionless) are effective moisture saturation in the surface and subsurface soil layers, λ is the exponential coefficient (>1) that expresses the impact of water saturation on evapotranspiration and interflow, c_4 and c_5 (cm day^{-1}) are coefficients for surface soil interflow and percolation, and C_{ti} is the effect of temperature on soil and water physical state. I_l and S_{ms} are expressed as:

$$I_l = (I_c/S_{ms}^{\gamma})C_{ti} \tag{11}$$

$$S_{ms} = (S3/S3_n - S_{rs})/(1{\cdot}0 - S_{rs}) \tag{12}$$

where I_c (cm day^{-1}) is an infiltration coefficient, γ is an exponential coefficient expressing the impact of water saturation on infiltration, $S3_n$ (cm) is the nominal surface soil storage, and S_{rs} is the minimum surface soil moisture saturation that can be attained.

The effect of temperature on infiltration is a complex phenomenon affected by the temperature fluctuation and the length of time the temperature stays above and below the active temperature. This phenomenon results in soil defrosting and refreezing. It is ignored by most of the existing models. This model assumes that the soil is defrosting exponentially with active temperature accumulation T_I. However, soil will be refrozen again if the temperature drops below zero for a number of days. The active temperature accumulation will be lost and will start again from zero. Hence, C_{ti} can be written as:

$$C_{ti} = \begin{cases} (T_I/T_{Imax})^{c_i} & \text{if} \quad T_I < T_{Imax} \\ 1 & \text{if} \quad T_I \ge T_{Imax} \end{cases} \tag{13}$$

$$T_I = \begin{cases} \sum T & \text{if} \quad T > 0 \quad \text{and} \quad N < N_n \\ 0 & \text{if} \quad N \ge N_n \end{cases} \tag{14}$$

$$N = \begin{cases} \sum N_0 & \text{if} \quad T < 0 \\ 0 & \text{if} \quad T \ge 0 \end{cases} \tag{15}$$

$$N_0 = \begin{cases} 1 & \text{if} \quad T < 0 \\ 0 & \text{if} \quad T \ge 0 \end{cases} \tag{16}$$

where T_{Imax} (°C) is a maximum T_I point at which surface soil is fully defrosted, c_i (dimensionless) is an exponent for describing the influence of T_I on soil defrosting, N (days) is the number of continuous days

with temperature below active point, N_n is a maximum N after which T_I will be lost and surface soil will refreeze again, N_0 is a logical variable to identify the day in which temperature is higher or lower than the active temperature.

Water in excess of the infiltration limit will route as overland flow R_{of}:

$$R_{of} = (\alpha T/C_1 + P_r) - R_{CI} - R_I \tag{17}$$

Subsurface soil storage sector. The source of moisture for the subsurface soil storage is from surface soil percolation, whereas the moisture losses are due to evapotranspiration R_{E2}, interflow R_{F2} and percolation to the groundwater storage R_{P2}. Rates of loss terms are determined by the subsurface soil water saturation (Manley, 1982). Vegetation cover and climatic conditions also influence evapotranspiration. Similar equations to those that describe the canopy interception capacity are developed for expressing vegetation as a function of active temperature accumulation. Hence, the following equations are used to describe moisture dynamics in subsurface soil storage:

$$\frac{dS4}{dt} = R_{P1} - R_{E2} - R_{F2} - R_{P2} \tag{18}$$

$$R_{E2} = c_6 T S_{mss}^{\lambda} C_{tc} \tag{19}$$

$$R_{F2} = c_7 S_{mss}^{\lambda} \tag{20}$$

$$R_{P2} = c_8 S_{mss}^{\lambda} \tag{21}$$

$$S_{mss} = (S4/S4_n - S_{rl})/(1{\cdot}0 - S_{rl}) \tag{22}$$

where $S4$ (cm) represents the water in subsurface soil storage, c_6 (cm $^{\circ}C^{-1}$ day^{-1}) is an evapotranspiration coefficient for the subsurface soil layer, c_7 and c_8 (cm day^{-1}) are coefficients for subsurface soil interflow and percolation, $S4_n$ (cm) stands for a nominal subsurface soil storage, and S_{rl} is the minimum subsurface soil moisture saturation that can be attained.

Groundwater storage sector. Groundwater storage is described as a linear shallow reservoir. Water enters the groundwater storage through percolation from the subsurface soil storage and comes out of this storage as baseflow to the stream. It is assumed that there exists a baseline groundwater level. The baseflow rate depends on the difference between the groundwater storage and the baseline groundwater level. Equations for the change in groundwater storage can be written as:

$$\frac{dS5}{dt} = R_{P2} - R_{BF} \tag{23}$$

$$R_{BF} = (S5 - S5_n)/c_9 \tag{24}$$

where $S5$ (cm) is the water in groundwater storage, R_{BF} (cm day^{-1}) stands for baseflow, $S5_n$ (cm) represents the baseline groundwater level and c_9 (day) is a coefficient for baseflow.

Runoff recession. Total water available R for routing as a runoff comes from the overland flow, the interflow from surface and subsurface storage as well as the baseflow from groundwater storage. It is given as:

$$R = R_{of} + R_{F1} + R_{F2} + R_{BF} \tag{25}$$

Streamflow response to the internal and/or external water availability is subject to the travel time delay. An average travel time is used in the model and a third-order exponential smooth function (High Performance

Systems, 1997) is selected by setting up a cascade of three first-order exponential relationships, each with an averaging time of time/3. Hence, streamflow Q can be calculated as:

$$Q = \mathrm{SMTH3}(RA, t_d, Q_i)r \tag{26}$$

where A (km^2) is the catchment area, r is a unit conversion coefficient (from cm km^2 day^{-1} to m^3 s^{-1}) with the value of 10 000/86 400, t_d (day) represents average delay time and Q_i stands for initial streamflow (cm km^2 day^{-1}). If an initial value for Q_i is not specified, SMTH3 assumes the value to be equal to the initial input value.

Model implementation. The model was developed and implemented using the STELLA II development tool (High Performance Systems, 1997). This modelling tool provides a user-friendly graphical interface. Under the STELLA environment, the modeller can use the basic building blocks to define the objects and the functional relationships. The basic graphical building blocks are stocks, flows, converters and connectors. Stocks are used to represent storage, which can be changed with flows. Flows are defined and regulated by converters. Converters are used to store algebraic relationships, define external input to the model and hold values for constants. Connectors function to connect model elements (stocks, flows and converters) and indicate the cause–effect relations. The model is represented by differential and difference equations that can be solved with either the Euler or Runge–Kutta method.

APPLICATION OF THE MODEL

Description of the study areas

The proposed system dynamics model has been applied for simulation of runoff in two river basins in Southern Manitoba, Canada: the Assiniboine River Basin and the Red River Basin (Figure 3).

The Assiniboine River originates in middle northwest Saskatchewan and drains the area from the eastern part of Saskatchewan to the western part of Manitoba. Its major tributaries include the Qu'Appelle River and Souris River. The Assiniboine River flows from northwest to southeast and joins the Red River in Winnipeg, Manitoba. The lower reach of the river is below the Shellmouth Dam, which can significantly reduce flow rates and downstream water levels. Therefore, this case study focuses on the Assiniboine River basin from headwaters to the Shellmouth Reservoir (Figure 3). The study area covers 16 496 km^2. Topographically, the basin is gently to moderately undulating with higher relief evident in the northeast portion. The northeast part of the basin is located within the boreal plains ecozone with brush and wooded bluffs cover and steeper flow gradient, whereas the southern part lies within the prairie ecozone, a flatter terrain characterized by less brush and fewer trees. Climatologically, the basin is continental sub-humid characterized by a long, cold winter and short, warm summer. The frost-free season varies from 90–110/days. Annual precipitation averages about 450 mm (with variations between 140 and 550 mm), of which 27% is snow. The streamflow in the basin is highly variable on a daily basis. During the springtime, water levels on the Assiniboine River are high due to the snowmelt. About 63% of annual total flow is contributed during the months of April and May, whereas this is only 3% during the period from December to March. Yearly flow variation is also high due to climate variations.

The Red River originates in Minnesota and flows north. It is located in the geographic centre of North America. The River enters Canada at Emerson, Manitoba, and continues northward to Lake Winnipeg. With the exclusion of the Assiniboine River and its tributaries, the Red River Basin covers 116 550 km^2, of which 103 600 km^2 is in the USA. The basin is remarkably flat and the slope of the river averages less than one-half foot per mile. The basin has a sub-humid to humid climate with moderately warm summers, cold winters and rapid changes in daily weather patterns. Annual precipitation is about 500 mm, with almost two-thirds occurring between May and July. Precipitation during the dry months from November to February averages

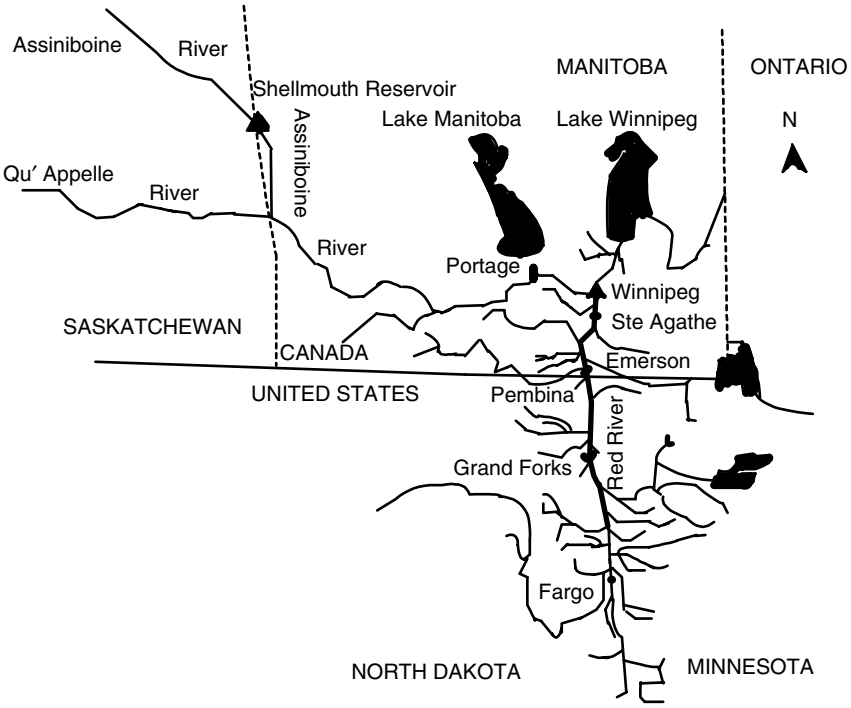

Figure 3. Study area and locations

only about 13 mm per month. Because the river flows from south to north, its southern reaches thaw before the lower river. Heavy snowfall and spring rains, coupled with late spring thaws, can cause the river to spill over shallow banks and across the floodplain, and result in incredible disasters (International Joint Commission, 2000).

Calibration and verification of the model

Flood flow records in both basins were divided for the purpose of model calibration and verification. The calibration process includes determining model parameters and initial values for all state variables. Calibration of parameters for the present study was performed by the trial- and error-method. Physically based parameters can be determined from the knowledge of catchment characteristics. Most hydrologic parameters can be obtained from the literature and field observations. Climate variables are retrieved from field observations. Those variables that could not be derived from the literature and field observations were calibrated through repeated simulation until a good match was obtained between calculated and observed flows. Statistical analysis was used for assessing the goodness-of-fit for guiding the calibration process (Aitken, 1973).

The initial values of the state variables used in the model are established from experience, as well as from the precipitation in previous fall and winter. Streamflow data were obtained from the Environment Canada Hydrological Database (HYDAT) and USGS real streamflow record database, and the climatic data were retrieved from the Environment Canada Climate Station Database and the American National Weather Service. In the Assiniboine River Basin, the flood of 1995 was used for calibration and the flood of 1979 for verification. Flows were measured at the entrance into the Shellmouth Reservoir. In the Red River Basin, the flood of 1996 was used in calibrations and the flood of 1997 in verification. Since the Red River flows from south to north through a wide span of geographic conditions in which there exist a great gradient in temperature and precipitation, dividing of the basin into several sub-catchments was required. Three sub-catchments were identified: (a) up to Grand Forks with 77 959 km^2; (b) between Grand Forks and Emerson

with 24 087 km^2; and from Emerson to Ste Agathe with 12 954 km^2. For each catchment, the differential and difference equations presented above are used to calculate streamflow. The following equations are used for streamflow calculations at Grand Forks, Emerson and Ste Agathe:

$$Q_1 = \mathrm{SMTH3}(R_1A_1, t_{\mathrm{d}1}, Q_{1\mathrm{i}})r \tag{27}$$

$$Q_2 = [\mathrm{SMTH3}(R_2A_2, t_{d2}, Q_{2\mathrm{i}}) + \mathrm{SMTH3}(R_1A_1, t_{\mathrm{d}1} + t_{12}, Q_{1\mathrm{i}})]r \tag{28}$$

$$Q_3 = [\mathrm{SMTH3}(R_3A_3, t_{\mathrm{d}3}, Q_{3\mathrm{i}}) + \mathrm{SMTH3}(R_2A_2, t_{d2} + t_{23}, Q_{2\mathrm{i}}) + \mathrm{SMTH3}(R_1A_1, t_{\mathrm{d}1} + t_{12} + t_{23}, Q_{1\mathrm{i}})]r \tag{29}$$

where Q_1, Q_2 and Q_3 (m^3 s^{-1}) represent simulated streamflow at Grand Forks, Emerson and Ste Agathe, R_1, R_2 and R_3 (cm day^{-1}) stand for total water available for routing as runoff at Grand Forks, Emerson and Ste Agathe, A_1, A_2 and A_3 are the catchment areas within Grand Forks, Emerson and Ste Agathe, $t_{\mathrm{d}1}$, $t_{\mathrm{d}2}$ and $t_{\mathrm{d}3}$ (day) represent average travel time within the Grand Forks catchment, Emerson catchment and Ste Agathe catchment, t_{12}, and t_{23} (day) are the average travel times from Grand Foks to Emerson and from Emerson to Ste Agathe, and $Q_{1\mathrm{i}}$, $Q_{2\mathrm{i}}$ and $Q_{3\mathrm{i}}$ (cm km^2 day^{-1}) stand for initial streamflow at Grand Foks, Emerson and Ste Agathe. The observed streamflow at Grand Forks, Emerson and Ste Agathe is used in model calibration and verification.

Model results

The input data set for model use includes all calibrated parameters, temperature, precipitation and a set of initial values for the state variables. Most of the parameters used in the model were given values (through the calibration process) within those available in the literature. The main parameters' relation to temperature and soil water capacity are shown in Table I.

Results: Assiniboine River. The simulated and measured streamflow data for the calibration year of 1995 and the verification year of 1979 in the Assiniboine River are shown in Figures 4 and 5. The results indicate that the simulated streamflow pattern is quite similar to that observed. In the case of the calibration flood year (Figure 4), the streamflow is smaller during the winter season due to the frozen surface soil. The active temperature starts in early March, which results in snowmelt and increase in streamflow. A small flow peak appeared during this snowmelt active period. From late March to early April, negative temperature lasted for about 2 weeks, which led to freezing of the surface soil again, and streamflow receded to the normal low level due to the absence of snowmelt. In mid-April, the temperature rose to the active point and snowmelt started again. As the temperature increased, more water was produced from snowmelt, and streamflow increased rapidly. In the meantime, the active temperature gradually defrosted the surface soil, which increased the infiltration rate and the surface soil storage capacity. More water infiltration into the surface soil increased water saturation, which, in turn, limited further water infiltration into the surface storage. Although the infiltration rate increased with increase in temperature, streamflow continued to increase due to the delay in snowmelt. Before the surface soil was fully defrosted, streamflow reached a peak in association with a rainfall in late April. Fully defrosted surface soil infiltrated most of the snowmelt water and reduced the streamflow. A lasting high active temperature gradually depleted accumulated snowpack before mid-May, and streamflow

Table I. Model calibration results

Catchment	α (cm °C^{-1} day^{-1})	$S3_{\mathrm{n}}$ (cm)	$S4_{\mathrm{n}}$ (cm)	T_{Imax} (°C)	T_{Cmax} (°C)	c_{c}	c_{i}	$C_{\max}$ (cm)
Assiniboine River	0·40	2·0	4·0	50	800	2·8	4·5	0·5
Red River	0·45	1·5	4·2	50	800	2·8	5·5	0·3

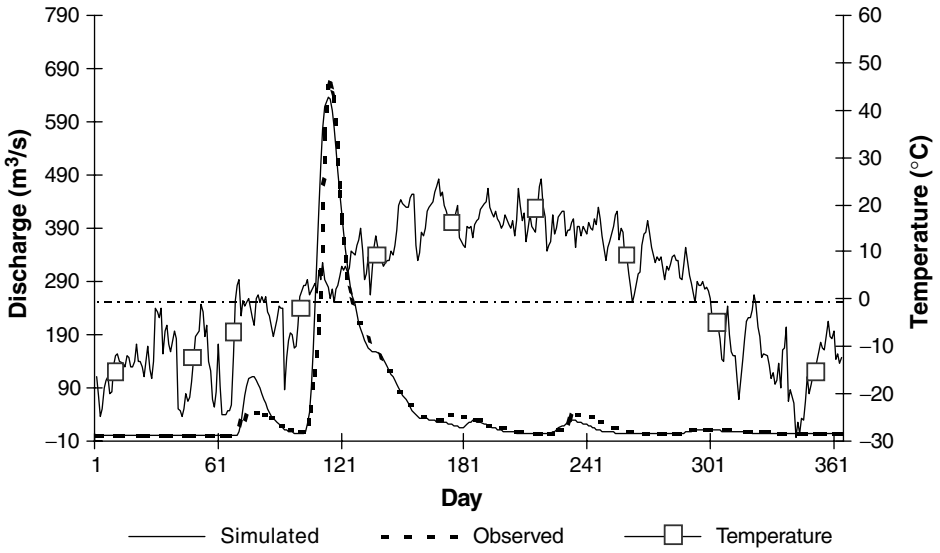

Figure 4. Simulated and measured streamflow in the Assiniboine River Basin for 1995 (calibration)

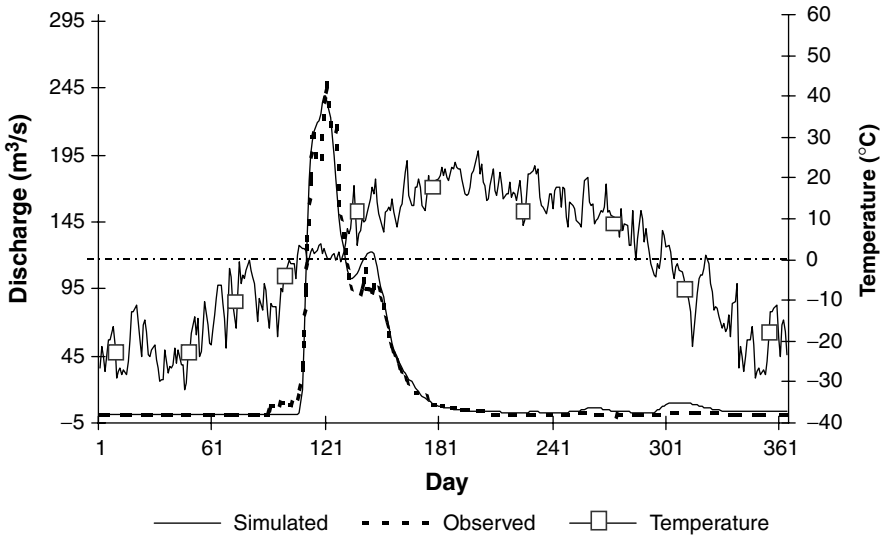

Figure 5. Simulated and measured streamflow in the Assiniboine River Basin for 1979 (verification)

returned to a normal level. After the snowmelt period, groundwater and soil storage again became the main contributors to streamflow, and fluctuations of streamflow were strongly dependent on the rainfall magnitude.

The moisture dynamics of the surface and subsurface soil layers and their response to precipitation are shown in Figure 6. In winter, the moisture content in the surface soil was stable because the surface soil was frozen, and losses were prevented from the soil. As the temperature reached the active point in early March, the surface soil started to thaw, and snowmelt water was infiltrated into the soil, which increased the moisture content. Moisture in the surface soil rapidly increased and remained at a high level after snowmelt started. More moisture in the surface soil resulted in an increase in subsurface soil moisture content with a time delay due to the percolation into the subsurface soil layer. More subsurface soil moisture also increased

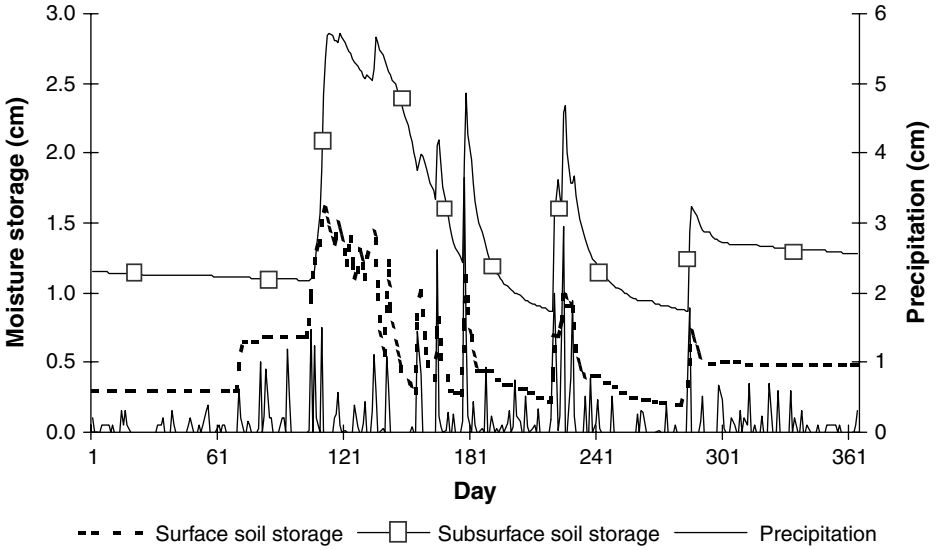

Figure 6. Moisture dynamics in the surface and subsurface storage in the Assiniboine River Basin in 1995

the water saturation, which reduced the percolation rate. After defrosting of the surface soil, moisture levels in the surface and subsurface soil layers remained at a high level because more water from the snowmelt entered into the surface soil, and high water saturation in the subsurface soil layer reduced the percolation. After the snowmelt period, the moisture in the surface soil was reduced and strong fluctuations that are caused by variation in rainfall magnitude started. After October, the temperature reached zero, and snowfall started to accumulate in the snowpack and the surface soil moisture level remained stable. Moisture accumulated in the surface soil during the fall is an important factor in the formation of the next year's flood. Figure 6 also indicates that the surface soil storage is a fast response component of the rainfall during the active temperature period, whereas the subsurface storage is a slow response component.

The verification results for the year 1979 also reproduced the flood starting time, peak and duration quite well (Figure 5). Simulated flow was underestimated at the beginning of April due to the temperature being below the active point. During the peak period, fluctuations in measured flow were observed, whereas simulated flow was smooth with only one peak. The influence of active temperature and its duration time on both the surface-soil defrosting and the snowmelt may be responsible for this difference. The model uses daily mean temperature to calculate snowmelt rate. In a real situation, temperature fluctuates during the day. During the snowmelt active period, temperature may change from negative to active within a day, and snowmelt may take place during the day and contribute water to streamflow. The duration of negative and active temperature also significantly influences the surface soil state and infiltration rate. The model did not capture daily fluctuations. However, the main purpose of the model is to assess the long-term behaviour and trends in streamflow, not daily changes. The model focuses on the comparison of the long-term trends and patterns from simulation and observation. In mid-May, the daily mean temperature rapidly reached about 20 °C, which produced more snowmelt water, resulting in an overestimation of flow in this period.

Results: Red River. Since the catchment area of the Red River Basin is very large, a division into three sub-catchments was done. The streamflow at the lower reach is routed together with the local inflow into the upper reach with a delay. Because the Red River flows north, its southern reaches thaw before these in the north. Flow in southern reaches significantly influences that in northern reaches. As a result, flood starting and peak times in northern reaches occur later than in southern reaches. Calibration and verification of the model for the Red River Basin show that this pattern was well reproduced and that the model captured the essential

dynamics of flows occurring in the basin. In the calibration flood year of 1996, simulated streamflow has matched observed flood pattern well during the snowmelt active period at Grand Forks: flood from snowmelt started and reached its peak in mid-April, and lasted about 30 days (Figure 7a). In late May, heavy rainfall resulted in a second peak. The flood pattern at Emerson and Ste Agathe is, to a great extent, determined by the pattern in the southern reaches with a time delay. Addition of snowmelt water in the lower reaches, meant that flow peaks at Emerson and Ste Agathe were higher than that at Grand Forks and the flood duration at Emerson and Ste Agathe was much longer than that at Grand Forks. This pattern was well reproduced by the model at Emerson and Ste Agathe (Figure 7b and c). However, the magnitude of the peak at Emerson was overestimated. At Ste Agathe, a second peak generated in late May was overestimated by the model. This peak was mainly generated by local heavy rainfall in the lower reaches of the river.

Figure 8 compares simulated and measured discharges for the verification flood year of 1997 (flood of the century) in the Red River Basin. At Grand Forks, predicted flood duration matched the observed one, but the peak magnitude is smaller than observed and the peak time is delayed. At the Emerson and Ste Agathe stations, peak magnitude and time matched those measured very well. After the snowmelt active period, there was a heavy rainfall in early July, which produced another streamflow peak. After July, streamflow remained at the normal level.

The model reproduced the basic dynamics of streamflow occurring in the watershed on a daily basis. The model does not capture the daily changes in temperature. Assiniboine River Basin is represented in the model in aggregated form. One set of parameters is used for the whole watershed. This aggregation ignores the spatial variation of climate, land use, mantle, and soil properties within the watershed. Although three sub-catchments are used in the Red River Basin, each sub-catchment contains a large area. The number and size of the sub-catchments for a watershed model depend on catchment characteristics, data availability and quality. For this reason, the combination of a system dynamics model with other tools, such as a geographical information system, may improve the presentation of spatially varying processes. A more detailed description of the catchment area and catchment soil properties may also improve the model performance.

Sensitivity analysis and statistical evaluation of results. Sensitivity analysis and assessment of goodness-of-fit are used to validate the model. Sensitivity analysis is performed by changing the value of one model parameter at a time. Cuenco *et al.* (1985) suggested varying the parameters by about ±10% of baseline value in sensitivity analysis. The response of streamflow to this variation is used for sensitivity evaluation in this study. In order to represent the dynamic characteristics of the streamflow, the following equations are used to calculate the sensitivity of model parameters:

$$\bar{s} = \frac{\sum_{t=1}^{n} \frac{Q'_{St} - Q_{St}}{Q_{St}}}{n} \times 100\% \tag{30}$$

$$s_p = \frac{Q'_{sp} - Q_{sp}}{Q_{sp}} \times 100\% \tag{31}$$

where $\bar{s}$ represents an averaged sensitivity of the streamflow to parameter variation, s_p is the sensitivity of the peak value, n is the length of time horizon, t is the time step, Q_{St} is the simulated streamflow that corresponds to the calibrated parameter value at time t, Q'_{St} is the streamflow corresponding to the modified parameter value, Q_{sp} and Q'_{sp} stand for the peak flow.

The reproduction of historical records is the most important test for evaluation of model performance. The goodness-of-fit of model results can be assessed by graphical and statistical tests. In order to measure the goodness-of-fit between simulated and observed data, three statistical measures are employed in this study: coefficient of efficiency R_E^2, coefficient of determination R_D^2 (the square of the correlation coefficient), and the

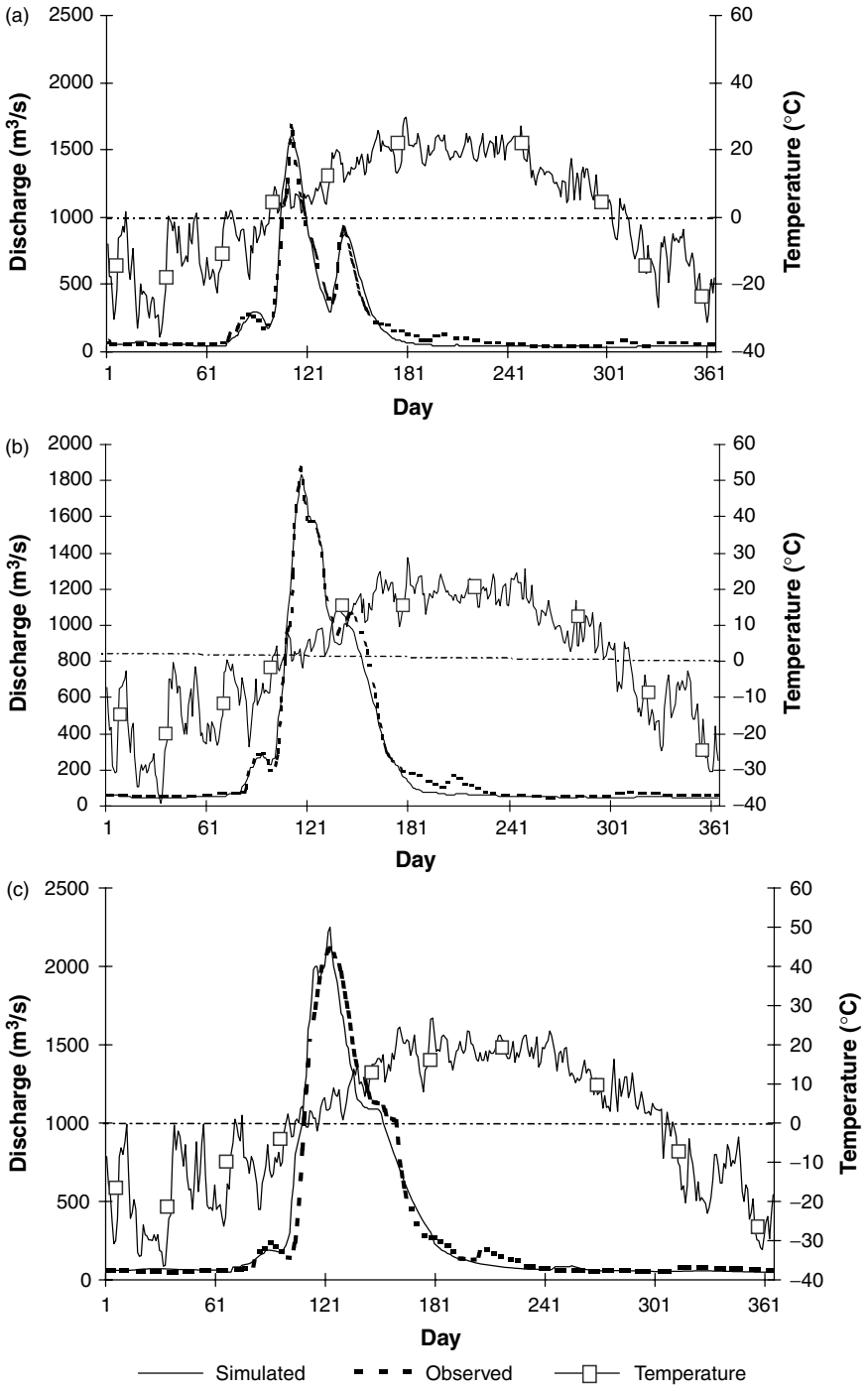

Figure 7. Simulated and measured streamflow in the Red River Basin for 1996 (calibration): (a) simulated and measured streamflow at Grand Forks; (b) simulated and measured streamflow at Emerson; (c) simulated and measured streamflow at Ste Agathe

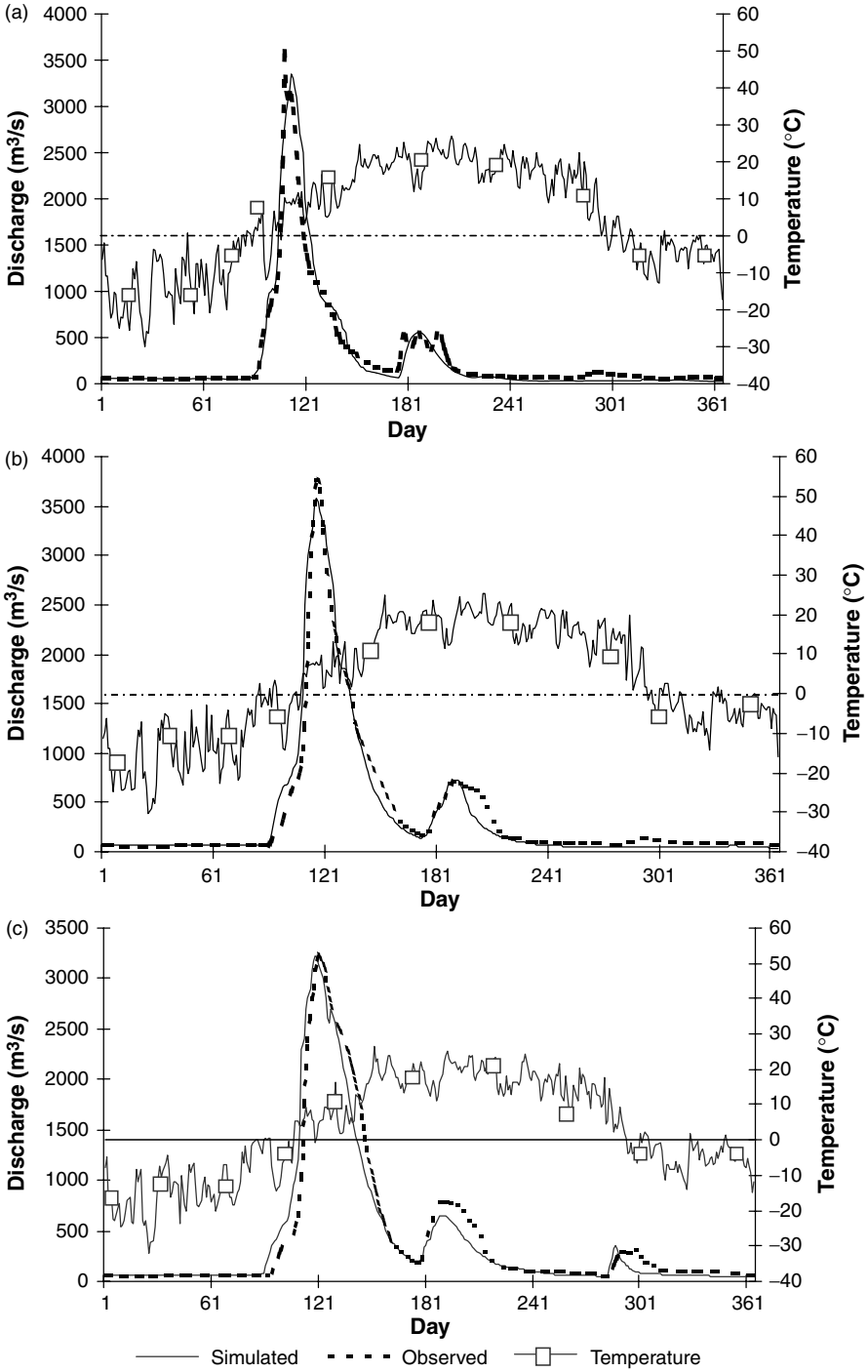

Figure 8. Simulated and measured streamflow in the Red River Basin for 1997 (verification): (a) simulated and measured streamflow at Grand Forks; (b) simulated and measured streamflow at Emerson; (c) simulated and measured streamflow at Ste Agathe

residual mass curve coefficient R_R^2. They can be calculated as:

$$R_E^2 = 1 - \left[\sum_{t=1}^{n}(Q_{St} - Q_{Mt})^2 \Big/ \sum_{t=1}^{n}(Q_{Mt} - \overline{Q}_M)^2\right] \tag{32}$$

$$R_D^2 = \left[\frac{\frac{1}{n}\left[\sum_{t=1}^{n}(Q_{St} - \overline{Q}_S)(Q_{Mt} - \overline{Q}_M)\right]}{S_{Q_S} S_{Q_M}}\right]^2 \tag{33}$$

$$R_R^2 = 1 - \left[\sum_{t=1}^{n}(D_{Mt} - D_{St})^2 \Big/ \sum_{t=1}^{n}(D_{Mt} - \overline{D}_M)^2\right] \tag{34}$$

where Q_{MSt} is the observed streamflow value at time t, $\overline{Q}_S$ and $\overline{Q}_M$ are the simulated and measured mean values, S_{Q_S} and S_{Q_M} are the standard deviations, D_{Mt} is the departure from the mean for the measured residual mass curve, D_{St} is the departure from the mean for the simulated residual mass curve, and $\overline{D}_M$ is the mean of the departures from the mean for the measured residual mass curve.

R_E^2 is a measure of the overall performance of the model, whereas R_D^2 and R_R^2 provide information concerning the systematic error in the model (Aitken, 1973; Putty and Prasad, 2000). In terms of assessing the historical fit of the model, the values of R_E^2, R_D^2, and R_R^2 should be high.

The calibration year is taken as a base case for the sensitivity analysis in both the Assiniboine River and Red River basins. Parameters related to the surface soil storage and the temperature were selected for sensitivity analysis. As shown in Table II, $\overline{s}$ and s_p are not sensitive to the selected-parameter variations. The influence of the selected-parameter variation on $\overline{s}$ is small (between −2·8% and +3·3%), whereas the influence of the selected-parameter variation on s_p varies. The variation in value of T_{Cmax}, c_c, and C_{max} has little influence on s_p. On the other hand, it looks as it s_p is much more sensitive to the variation in α and T_{Imax} (for change of T_{Imax} the s_p value varies from −13·0% to +12·5% in the Assiniboine River Basin). The results show that snowmelt and soil defrosting are the most important factors for flood peak generation. This is consistent with the assumptions established at the beginning of this study. More detailed study of the temperature impact on the snowmelt and soil defrosting could improve the prediction of floods in the case study area.

Table II. Sensitivity analysis of the model (%)

Parameter Change		Assinboine River		Red River Basin					
				at Grand Forks		at Emerson		at Ste Agathe	
	(%)	$\overline{s}$	s_p	$\overline{s}$	s_p	$\overline{s}$	s_p	$\overline{s}$	s_p
α	−10	−2·36	−8·29	−0·92	−6·11	−1·15	−5·96	−1·45	−6·81
	+10	2·62	8·49	0·85	4·88	1·20	5·19	1·46	6·33
$S1_n$	−10	0·75	6·45	−0·23	0·89	−0·39	0·85	−0·30	1·05
	+10	−0·57	−4·19	−0·31	−0·95	−0·24	−0·92	−0·35	−1·11
T_{Imax}	−10	0·31	−12·97	−0·09	−4·13	−0·23	−3·92	−0·36	−4·57
	+10	−0·14	12·50	0·14	3·65	0·25	3·46	0·36	4·26
T_{Cmax}	−10	−2·09	0·00	−0·55	0·00	−0·51	0·00	−0·46	0·00
	+10	2·17	0·00	0·58	0·00	0·56	0·00	0·53	0·00
c_c	−10	−1·24	0·00	−0·31	−0·01	−0·28	−0·01	−0·24	−0·01
	+10	1·09	0·00	0·26	0·00	0·24	0·00	0·20	0·00
c_i	−10	1·72	−7·92	0·01	−0·88	−0·03	−0·86	−0·06	−1·12
	+10	−1·58	5·48	−0·01	0·76	0·02	0·72	0·05	0·95
C_{max}	−10	3·35	0·23	2·38	0·02	2·68	0·02	2·48	0·03
	+10	−2·82	−0·23	−2·24	−0·02	−2·45	−0·02	−2·29	−0·03

Graphical comparison in Figures 4, 5, 7 and 8 shows that simulated values are properly reproducing the pattern of floods in the case study area. More rigorous statistical assessment of the goodness-of-fit is made and summarized in Table III. The model-simulated mean and standard deviation are close to these measured, and the R_E^2 is high (0·89 to 0·97). Therefore, the model overall performance is judged to be good. Simulated peak values are close to these measured. The difference between the simulated and the observed peak flow at all locations is below 4% except at Grand Forks in the 1997 verification year (6·7%). The degree-day factor may be responsible for this exception. According to Warkentin's (1999) calculation, the average degree-day factor at Grand Forks during the active snowmelt period in 1997 was higher than that in the calibration year of 1996. The comparison of the magnitude of R_D^2 and R_R^2 revealed that the error is unsystematic and random, and that the model can catch the essential dynamics of the streamflow and moisture movement in the surface and the subsurface layers.

In summary, the calibration and the verification of the model for the Assiniboine River and the Red River showed that the simulated streamflow stays within the bounds of measurement error, and fit the measured data quite well. The model captures the most important hydrologic dynamics and can be used efficiently to extrapolate and predict flood patterns caused by the climatic change and variation.

CONCLUSION

Snowpack accumulation and snowmelt are found to have a major importance on flood generation in the North American prairies. Temperature is a critical climate factor to distinguish between the snowfall and the rainfall, and to determine the snowmelt rate and the physical state of soil. Previous hydrological models have incorporated the climate factors, land use and soil properties to estimate the streamflow, but they have not explicitly represented the internal hydrologic dynamics and the impact of climate factors on them. This study uses a system dynamics approach to explore the hydrologic processes in situations where floods are significantly contributed to by snowmelt. System dynamics provides an effective modelling methodology for organizing and integrating existing information available on the hydrologic processes in a watershed system, especially temperature and precipitation data available from observations and the predictions of global climate models. The model proposed in this study closely follows the dynamic processes of the hydrologic cycling in a watershed. The model clarifies both the interactions among the surface–subsurface storage and the role of temperature change on the canopy size, soil physical state and flood generation. The model has defined a clear boundary, i.e. the model explained the key variables required to generate the hydrological behaviour. Dynamic behaviour of the streamflow is generated by the internal feedback structure and the strong external disturbance.

Table III. Error analysis of the hydrological model

Catchment	Year	Mean ($m^3\ s^{-1}$)		Standard deviation		Peak value ($m^3\ s^{-1}$)		R_E^2	R_D^2	R_R^2
		$\overline{Q}_M$	$\overline{Q}_S$	S_{Q_M}	S_{Q_S}	Q_{MP}	Q_{SP}			
Assiniboine River	1995	43·69	46·12	102·20	108·86	661·00	637·49	0·93	0·94	0·93
	1979	19·89	22·62	47·62	50·34	248·60	239·61	0·95	0·96	0·96
Red River										
Grand Forks	1996	187·36	184·07	281·75	307·18	1628·80	1678·60	0·95	0·96	0·95
	1997	291·09	284·62	540·60	624·30	3596·24	3355·88	0·88	0·92	0·88
Emerson	1996	257·25	258·04	411·07	418·95	1869·12	1936·00	0·96	0·97	0·96
	1997	371·83	361·62	670·65	738·29	3766·56	3773·25	0·94	0·96	0·94
Ste Agathe	1996	310·32	332·33	515·49	512·44	2113·30	2166·55	0·96	0·96	0·96
	1997	413·19	420·49	717·76	748·57	3230·00	3345·35	0·97	0·97	0·97

The performance of the hydrological model shows that the simulated streamflow reflects the variation in temperature and precipitation as well as the moisture interaction between the surface, subsurface and the groundwater storages. Comparison of the results from simulation and observation indicates that the model can reproduce well the observed flood starting time, peak and the duration. Statistical analysis revealed that the error is unsystematic and the model quantitatively matches the historical data. The model in its present form provides a yearly prediction of streamflow on a daily basis. The model can be used to make a long-term prediction of streamflow under different climate change scenarios. If the model is used to make precise predictions of flood events for a short term, daily variations in temperature and precipitation should be taken into account. Meanwhile, the model lumped structure ignores the spatial variation of climate, mantle and soil properties. Further studies to refine the hydrologic dynamics by taking spatial variations into account are warranted to improve the model's ability to reproduce historic data and to predict future flood events.

ACKNOWLEDGEMENTS

This work was made possible by financial support from Natural Resources Canada through the Climate Change Action Fund. The authors would like to thank Environment Canada for providing climate and streamflow records, the department of Water Resource, Manitoba Conservation for providing watershed characteristics, the Minnesota Climatologic Working Group for creating a gateway to access National Weather Service data, and the USGS for the streamflow records.

APPENDIX A

List of symbols

α	degree-day factor for snowmelt
λ	exponential coefficient for evapotranspiration and interflow
γ	exponential coefficient for water saturation influence on infiltration
A, A_1, A_2, A_3	catchment area
c_1	snow-water equivalent coefficient
c_2, c_3, c_6	evapotranspiration coefficient for canopy, surface and subsurface soil
c_4, c_7	surface and subsurface soil interflow coefficient
c_5, c_8	surface and subsurface soil percolation coefficient
c_9	coefficient for baseflow
c_c, c_i	exponential coefficient of active temperature accumulation on the canopy growth and soil defrosting
C_{CI}	canopy interception capacity
C_{max}	maximum C_{CI}
C_{min}	minimum part of C_{max} in winter
C_{tc}, C_{ti}	influence of temperature on the canopy size and soil physical state
$\overline{D}_M$	mean of the departures from the mean for measured residual mass curve
D_{Mt}, D_{St}	departure from the mean for measured and simulated residual mass curve
I_l, I_c	soil infiltration limit and coefficient
n	length of time horizon
N	number of continuous days with temperature below active point
N_0	logical variable identifying daily temperature greater or less than 0 °C
N_n	maximum N for active temperature accumulation
P_s, P_r	precipitation as snowfall and rainfall
Q, Q_1, Q_2, Q_3	streamflow in catchments

Q_{i}, $Q_{1\mathrm{i}}$ $Q_{2\mathrm{i}}$, $Q_{3\mathrm{i}}$	initial streamflow
$\overline{Q}_{\mathrm{S}}$, $\overline{Q}_{\mathrm{M}}$	mean streamflow from simulation and observation
Q_{MP}, Q_{sp}, Q'_{sp}	peak streamflow from measurement, simulation and sensitivity analysis
$Q_{\mathrm{S}t}$, $Q_{\mathrm{M}t}$	simulated and measured streamflow at time t
$Q'_{\mathrm{S}t}$	streamflow from sensitivity analysis
r	unit conversion coefficient
R, R_1, R_2, R_3	total water available for routing as a runoff in catchments
R_{BF}	baseflow rate
R_{CI}	canopy interception rate
R^2_{D}	coefficient of determination
R_{E1}, R_{E2}	evapotranspiration rate from surface and subsurface soil layer
R^2_{E}	coefficient of efficiency
R_{F1}, R_{F2}	interflow rate from surface and subsurface soil layer
R_I	infiltration rate
R_{of}	overland flow rate
R_{P1}, R_{P2}	percolation rate from surface and subsurface soil layer
R^2_{R}	residual mass curve coefficient
$\overline{s}$, s_{p}	averaged sensitivity and peak value sensitivity
$S1$	snow storage
$S2$, $S3$, $S4$, $S5$	water in canopy, surface soil, subsurface soil and groundwater storage
$S3_{\mathrm{n}}$, $S4_{\mathrm{n}}$	nominal surface and subsurface soil storage
$S5_{\mathrm{n}}$	baseline groundwater level
S_{ms}, S_{mss}	effective moisture saturation in surface and subsurface soil layer
$S_{Q_{\mathrm{S}}}$, $S_{Q_{\mathrm{M}}}$	standard deviations of streamflow from simulation and observation
S_{rs}, S_{rl}	minimum surface and subsurface soil moisture saturation
T	daily mean temperature
t	time step
$T_{C_{\max}}$, T_{Imax}	maximum T_{I} for canopy capacity and soil defrosting
t_{d}, t_{d1}, t_{d2}, t_{d3}	average delay time
t_{12}, t_{23}	average travel time of streamflow from one catchment to another
T_I	active temperature accumulation

REFERENCES

Aitken AP. 1973. Assessing systematic errors in rainfall-runoff models. *Journal of Hydrology* **20**: 121–136.

Anderson EA. 1973. *National Weather Service River Forecast System—Snow Accumulation and Ablation Model*. NOAA Tech. Memo. NWS HYDRO-17, US Dept Commerce, Washington, DC, USA.

Arp PA, Yin X. 1992. Prediction water fluxes throughout forests from monthly precipitation mean monthly air temperature records. *Canadian Journal of Forest Research* **22**: 864–877.

Beven K. 2001. How far can we go in distributed hydrological modelling? *Hydrology and Earth System Sciences* **5**(1): 1–12.

Bicknell BR, Imhoff JC, Kittle JL Jr, Donigian AS Jr, Johanson RC. 1997. *Hydrological Simulation Program—Fortran: User's Manual for Version 11*. US Environmental Protection Agency, National Exposure Research Laboratory, Athens, GA, EPA/600/R-97/080, 755.

Bobba AG, Lam DCL. 1990. Hydrological modeling of acidified Canadian watersheds. *Ecological Modeling* **50**: 5–32.

Cuenco ML, Stickney R, Grant WE. 1985. Fish bioenergetics and growth in aquaculture ponds: I. Individual fish model development. *Ecological Modeling* **27**: 169–190.

Danish Hydraulic Institute. 1992. *MIKE 11 Flood Forecasting Reference Manual*.

Ehrman JM, Higuchi K, Clair TA. 2000. Backcasting to test the use of neural networks for predicting runoff in Canadian rivers. *Canadian Water Resources Journal* **25**(30): 279–291.

Forester JW. 1968. *Principles of Systems*, 2nd edn. Productivity Press: MA.

Gray DM, Male DH. 1981. *Handbook of Snow*. Pergamon Press: New York.

Gutierrez LT, Fey WR. 1980. *Ecosystem Succession: A General Hypothesis and Test Model of a Grassland*. MIT Press: Cambridge, MA.

High Performance Systems, Inc. 1997. *Technical Documentation—STELLA*; 255 pp.

Hsu KL, Gupta HV, Sorooshian S. 1995. Artificial neural network modelling of the rainfall-runoff process. *Water Resources Bulletin* **25**: 483–490.
International Joint Commission. 2000. *Living with the Red, a Report to the Government of Canada and the United States on Reducing Flood Impacts in the Red River Basin*. IJC: Ottawa and Washington; 273 pp.
Jakeman AJ, Hornberger GM. 1993. How much complexity is warranted in a rainfall-runoff model? *Water Resources Research* **29**: 2637–2649.
Kite GW. 1998. *Manual for the SLURP Hydrological Model*, V. 11. National Hydrology Research Institute: Saskatoon; 159 pp.
Kite GW, Dalton A, Dion K. 1994. Simulation of streamflow in a macroscale watershed using general circulation model data. *Water Resources Research* **30**: 1547–1559.
Lealand CM, Born SH, Simonovic SP. 1999. Short-term streamflow forecasting using artificial neural network. *Journal of Hydrology* **214**: 32–48.
Leavesley GH, Lichty RW, Troutman BM, Saindon LG. 1983. Precipitation-runoff modeling system: user's manual. US Geological Survey Water-Resources Investigations Report 83-4238, 207.
Lindström G, Johansson B, Persson M, Gardelin M, Bergström S. 1997. Development and test of the distributed HBV-96 hydrological model. *Journal of Hydrology* **201**: 272–288.
Manley RE. 1982. *HYSIM—a General Purpose Hydrologic Model, Pisa Symposium 1978*. Pergamon Press.
Martinec J. 1960. The degree-day factor for snowmelt runoff forecasting. In *IUGG General Assembly of Helsinki, IAHS Commission of Surface Waters*. IAHS Publ. No. 51, IAHS: Wallingford; 468–477.
Martinec J. 1970. Study of snowmelt runoff process in two representative watersheds with different elevation range. In *Symposition on the Results of Research on Representative and Experimental Basins. Wellington 1970*. IAHS Publ. No. 96 IAHS/UNESCO: 29–39.
Martinec J. 1975. Snowmelt-runoff model for stream flow forecasts. *Nordic Hydrology* **6**(3): 145–154.
Martinec J, Rango A, Major E. 1983. *The Snowmelt-Runoff Model (SRM) User's Manual*. NASA Reference Publication 1100, Washington, DC; 118 pp.
Putty MRY, Prasad R. 2000. Understanding runoff processes using a watershed model—a case study in the Western Ghats in South India. *Journal of Hydrology* **228**: 215–227.
Richardson GP. 1991. *Feedback Thought in Social Science and Systems Theory*. University of Pennsylvania Press: Philadelphia, PA.
Rumelhardt DE, McLelland JL. 1986. *Parallel Distributed Processing Explorations in the Microstructure of Cognition*. MIT Press: Cambridge, MA.
Senge PM. 1990. *The Fifth Discipline*. Doubleday: New York.
Singh P, Kumar N. 1996. Determination of snowmelt factor in the Himalayan region. *Hydrological Science Journal* **41**: 301–310.
Thomas RB, Megahan WF. 1998. Peak flow responses to clear-cutting and roads in small and large basins, Western Cascades, Oregon: a second opinion. *Water Resources Research* **34**: 3393–3403.
US Army Corps of Engineers. 1971. Runoff evaluation and streamflow simulation by computer. Part-II. US Army Corps of Engineers. North Pacific Division, Portland, OR, USA.
Warkentin AA. 1999. *Red River at Winniepg—hydrometeorological parameter generated floods for design purposes*. Report of Manitoba Water Resources, Winnipeg, Canada, 32 pp.
World Meteorological Organization. 1970. *Guide to hydrometeorological practices*. WMO-No. 168. TP.82, Geneva, Switzerland.

